Molecular Cancer Therapeutics

Genipin Enhances the Therapeutic Effects of Oxaliplatin by Upregulating BIM in Colorectal Cancer

Bo Ram Kim[1], Yoon A. Jeong[2], Min Jee Jo[2], Seong Hye Park[2], Yoo Jin Na[2], Jung Lim Kim[1], Soyeon Jeong[1], Hye Kyeong Yun[2], Sanghee Kang[3], Dae-Hee Lee[1], and Sang Cheul Oh[1]

Abstract

Despite an increase in the survival rate of patients with cancer owing to the use of current chemotherapeutic agents, adverse effects of cancer therapies remain a concern. Combination therapies have been developed to increase efficacy, reduce adverse effects, and overcome drug resistance. Genipin is a natural product derived from *Gardenia jasminoides*, which has been associated with anti-inflammatory, anti-angiogenic, and anti-proliferative effects; hypertension; and anti-ischemic brain injuries. However, the enhancement of oxaliplatin sensitivity by genipin remains unexplored. Our study showed that a combination of genipin and oxaliplatin exerts synergistic antitumor effects *in vitro* and *in vivo* in colorectal cancer cell lines through the reactive oxygen species (ROS)/endoplasmic reticulum (ER) stress/BIM pathway. Importantly, the combination did not affect normal colon cells. BIM knockdown markedly inhibited apoptosis induced by the combination. In addition, genipin induced ROS by inhibiting superoxide dismutase 3 activity. These findings suggest that genipin may be a novel agent for increasing the sensitivity of oxaliplatin against colorectal cancer. The combination of oxaliplatin and genipin hold significant therapeutic potential with minimal adverse effects.

Introduction

Colorectal cancer is the third most frequently occurring disease and the fourth leading cause of cancer-related death worldwide (1). Although the survival rate of patients with colorectal cancer has increased recently, it is still lower than that of patients with other cancers. The five-year survival rate of patients with metastatic colorectal cancer is reported to be less than 10% (2). Colorectal cancer patients are usually treated with surgery, chemotherapy, and radiotherapy. 5-Fluorouracil, oxaliplatin, and irinotecan are commonly used for chemotherapy; however, they are associated with poor efficacies, high toxicities, and several adverse effects. In addition, numerous patients with distant metastasis or stage II and III colorectal cancer do not respond to adjuvant chemotherapeutic regimens (3, 4). Therefore, combination therapies with increased efficacies and reduced adverse effects are being developed to overcome drug resistance (5). Thus, novel agents are needed to enhance chemotherapeutic efficacy and decrease adverse effects.

Oxaliplatin is a third-generation platinum drug that is less toxic than cisplatin. The cytotoxicity of oxaliplatin is primarily due to the formation of platinum-DNA adducts that inhibit DNA replication and transcription. As a result, various signaling pathways are activated to induce DNA repair and cell death (6, 7). When oxaliplatin was first used in the early 2000s, the chemotherapy of metastatic colorectal cancer and the survival rate of patients with colorectal cancer were significantly enhanced. It is currently used together with 5-fluorouracil and folinic acid (FOLFOX) to treat colorectal cancer (8, 9). However, it exhibits dose-dependent clinical toxicity, and needs to be combined with another chemotherapeutic agent to minimize adverse effects and maximize treatment efficacy.

Genipin is a natural product derived from *Gardenia jasminoides* (10, 11). It exerts anti-inflammatory, anti-angiogenic, anti-proliferative, hypertension, anti-ischemic brain injuries, and regulates the Hedgehog signaling pathway (12–14). We previously demonstrated that genipin exerts an antitumor effect by inhibiting the Hedgehog signaling pathway in colorectal cancer (15). However, the mechanism of genipin-induced enhancement in oxaliplatin sensitivity is unknown. Therefore, we hypothesized that a genipin-mediated increase in oxaliplatin sensitivity induces apoptosis in colorectal cancer.

In this study, we investigated whether genipin sensitizes colorectal cancer cells to oxaliplatin-induced apoptosis. Notably, at non-cytotoxic concentrations, genipin or oxaliplatin efficiently induced cell death via a combined effect in colorectal cancer cell lines. We demonstrate for the first time that genipin enhances oxaliplatin-mediated apoptosis through the upregulation of BIM and intrinsic apoptosis pathways. We show that genipin increases Bak and BIM activities. In addition, we confirmed that genipin-mediated reactive oxygen species (ROS) generation increases the sensitivity of oxaliplatin by down-regulating extracellular superoxide dismutase 3 (SOD3). Collectively, our data suggest that

[1]Department of Oncology, Korea University Guro Hospital, Korea University College of Medicine, Seoul, Republic of Korea. [2]Graduate School of Medicine, Korea University College of Medicine, Seoul, Republic of Korea. [3]Department of Surgery, Korea University Guro Hospital, Korea University College of Medicine, Seoul, Republic of Korea.

Note: Supplementary data for this article are available at Molecular Cancer Therapeutics Online (http://mct.aacrjournals.org/).

B.R. Kim and Y.A. Jeong contributed equally to this article.

Corresponding Authors: Dae-Hee Lee, Korea University, Seoul 08308, Republic of Korea (South); Phone: 82-10-3929-1569; E-mail: neogene@korea.ac.kr; and Sang Cheul Oh, Korea University, Seoul 08308, Republic of Korea (South); Phone: 82-10-3006-7871; E-mail: sachoh@korea.ac.kr

doi: 10.1158/1535-7163.MCT-18-0196

genipin enhances the therapeutic effects of oxaliplatin by upregulating BIM in colorectal cancer cells.

Materials and Methods

Cell culture

Human colorectal cancer cell lines, HCT116, and DLD-1 were purchased from the ATCC. Cells were cultured in RPMI-1640 medium (Invitrogen) with 10% FBS (HyClone), 1 mmol/L L-glutamine, and 26 mmol/L sodium bicarbonate for monolayer cell culture. Human normal colon (CCD18CO) and lung (BEAS-2B) cell lines were purchased from the ATCC. All cell lines were grown at 37°C in a humidified chamber with 5% CO_2.

Reagents and antibodies

Genipin was purchased from Calbiochem. JNK inhibitor was purchased from Calbiochem (16, 17). Oxaliplatin was purchased from Sigma-Aldrich. Anti-Bak, anti-Bcl-2, anti-Mcl-1, anti-Bcl-Xl, anti-p53, anti-SOD3, anti-CHOP, anti-SMO, anti-PTCH, and anti-Nitrotyrosine (3NT) antibodies were purchased from Santa Cruz Biotechnology. Anti-XIAP, anti-NOXA, anti-BIM, anti-survivin, anti-Bid, anti-phospho JNK, anti-IRE1α, anti-phospho IRE1α, anti-Bip, anti-GRP94, anti-ATF6, anti-eIF2α, anti-phospho eIF2α, anti-XBP1s, anti-SOD2, anti-SOD1, anti-catalase, anti-NOX4, anti-NOX2, anti-cleaved PARP, anti-caspase-3, anti-caspase-9, and anti-Gli-1 antibodies were purchased from Cell Signaling Technology. Anti-SHH and anti-4 Hydroxynonenal (4-HNE) were from Abcam. Anti-Actin antibody was purchased from Sigma-Aldrich. For the secondary antibodies, anti-mouse IgG HRP and anti-rabbit IgG HRP were purchased from Cell Signaling Technology.

In vitro bioluminescence detection

HCT116 cells express luciferase. Thus, luciferase activity was confirmed by seeding 12-well plates with HCT116 cells. Next, they were treated with 10 μmol/L oxaliplatin, 100 μmol/L genipin, or their combination for 24 hours. The cells were then treated with 50 mg/mL of D-luciferin (Biovision, Cat. No. 7903). Luciferase signals were measured by using NightOWL LB983 *in vivo* bioluminescence imaging (BLI) system (Berthold Technologies) for 10 seconds.

Western blotting

Cells were lysed in RIPA buffer (50 mmol/L Tris, 150 mmol/L NaCl, 1% Triton X-100, 0.1% SDS, and 1% Na deoxycholate [pH 7.4]) with a protease and phosphatase inhibitor cocktail (Sigma-Aldrich). Protein concentrations were measured using the bicinchoninic acid protein assay reagent (Thermo Fisher Scientific). Equal amounts of proteins were separated by SDS-PAGE and transferred to nitrocellulose membranes (GE Healthcare Life Sciences). The membranes were blocked with TBS containing 0.2% Tween 20 and 5% skim milk, incubated with primary antibodies overnight at 4°C, and then incubated with horseradish peroxidase (HRP)–labeled secondary antibodies. The signals were detected by X-ray film.

Flow cytometry analysis of cell apoptosis

The translocation of phosphatidylserine, an apoptosis marker, from the inner to the outer leaflet of the plasma membrane was detected by the binding of allophycocyanin-conjugated annexin V. Briefly, HCT116 cells untreated or treated with genipin, oxaliplatin, or a combination of the two agents were resuspended in the binding buffer provided with the Annexin V-FITC Apoptosis Detection Kit (BioBud, Cat. No. LS-02-100). Cells were mixed with 1.25 μL Annexin V- 7 μL PI reagent and incubated for 30 minutes at 4°C in the dark. The staining was then terminated and cells were immediately analyzed by flow cytometry.

BIM or SOD3 overexpression

Cells were transfected with human BIM tagged with pDDK-Myc or SOD3 tagged with pDDK-Myc using a vector (Origene, Cat. No. RC2057559 or Cat. No. 204156). Cells were transfected with 1 μg DNA of pDDK-Myc BIM or pDDK-Myc SOD3 using Lipofectamine 2000 (Invitrogen), according to the manufacturer's instructions. After 24 hours of transfection, the cells were treated with oxaliplatin for further analysis.

Small interfering RNA

BIM siRNA (Cat. No. SC-29802) and negative control siRNA (Cat. No. SC-37007) were purchased from Santa Cruz Biotechnology. Cells were transfected with siRNA oligonucleotides using Lipofectamine RNAi Max reagents (Invitrogen) according to the manufacturer's instructions.

ROS measurement

ROS generation was measured by using dihydroethidium (Thermo Fisher Scientific). Cells were incubated for 30 minutes with 10 μmol/L dihydroethidium (DHE). Furthermore, the cells were washed with PBS, and fluorescence intensity was analyzed using a flow cytometer.

Immunofluorescence staining

Cells grown on glass coverslips were fixed with 3.7% formaldehyde for 15 minutes, followed by permeabilization with 0.5% Triton X-100 for 15 minutes at room temperature. Cells were then blocked for 1 hour with 3% BSA and probed with primary antibodies overnight at 4°C, followed by incubation with secondary Alexa fluor-594-conjugated secondary antibody (Molecular Probes) or FITC-conjugated secondary antibody (Sigma-Aldrich). The nuclei were co-stained with DAPI. The cells were mounted in Vectashield mounting medium (Vector laboratories) and visualized by fluorescence microscopy.

Tumor xenograft experiment

All animal experiments were carried out in accordance with animal care guidelines approved by the Korea University Institutional Animal Care and Use Committee (IACUC). Four-week-old female BALB/c nude mice were acquired from Orient Bio (Korea) and housed in a specific pathogen-free environment. The animals were acclimated for one week prior to the study and were provided open access to food and water. HCT116-Luc cells (3×10^6) in 100 μmol/L of culture medium were mixed with 100 μmol/L of Matrigel and implanted subcutaneously into 5-week-old BALB/c nude female mice. The tumor size was measured every 2 days.

In vivo bioluminescence imaging

The animals underwent imaging at a peak time of 3 minutes after intraperitoneal injection of D-luciferin (100 mg/kg) via NightOWL LB983 *in vivo* bioluminescence imaging (BLI) system (Berthold Technologies). Images were processed using the *in vivo* Image software (IndiGO) by counting the total number of photons per second for tumor regions of interest.

Immunohistochemistry staining and scoring

Sections of formalin-fixed, paraffin-embedded tumor specimens were deparaffinized in xylene and hydrated in a graded alcohol series. Endogenous peroxidase was blocked using 3% hydrogen peroxide in distilled water for 15 minutes, and antigen retrieval was performed by heating at 100°C for 20 minutes. The tissue slides were incubated with a universal blocking solution for 15 min at room temperature, then incubated at 4°C overnight with primary antibodies. The antibodies, catalog number, and dilutions used in this method are listed in Table 1. The samples were incubated with peroxidase-conjugated anti-goat IgG for 1 hour at room temperature. Immunohistochemistry (IHC) reactions were visualized by diaminobenzidine staining using the EnVision + system (Dako). Three investigators (Y.A. Jeong, J.L. Kim, and B.R. Kim) independently interpreted SOD3 and BIM staining under a light microscope; when they observed nuclei or membrane staining, they recorded the stained cells as positive. The staining intensity was divided into 5 grades, as shown in Table 2.

Terminal deoxyribonucleotidyltransferase–mediated deoxyuridine triphosphate nick end labeling (TUNEL) staining

TUNEL staining was performed using the *in situ* cell death detection kit TMR red (ROCHE; Cat. No. 12156792910) according to the manufacturer's instructions.

Statistical analysis

GraphPad InStat 6 software was used for all statistical analyses (GraphPad Software, Inc.). Statistics were analyzed by using one-way ANOVA with GraphPad InStat 6. One-way ANOVA followed by Turkey *post hoc* tests were performed in all statistical analysis. To determine the significance between two groups, an unpaired *t* test was used, where a *P* value of less than 0.05 was considered significant.

Results

Genipin enhanced oxaliplatin sensitivity in colorectal cancer cells but not in normal primary colon cells

First, we performed the MTT assay to detect cell viability after oxaliplatin exposure in colorectal cancer cell lines. Oxaliplatin induced cell death in a dose-dependent manner in colorectal cancer cells, but not in CCD-18Co normal primary colon cells (Fig. 1A). To investigate whether genipin could enhance oxaliplatin-induced apoptosis, we treated cells with genipin for 24 hours before analyzing cell viability by the MTT assay. Genipin induced cell death in a dose-dependent manner in colorectal cancer cells, but not in CCD-18Co normal primary colon cells (Fig. 1B and C). The combination of oxaliplatin and genipin significantly enhanced cell death as indicated by trypan blue staining in colorectal cancer cell lines (HCT116, DLD-1, SNU283, and HT29; Fig. 1E). However, normal primary colon cells (CCD-18Co) and normal lung cells (BEAS-2B) were not affected (Fig. 1D; Supplementary Fig. S1A). We also investigated geniposide, an analogue of genipin, to determine whether cell death occurred via a combined effect in colorectal cancer cells. Unlike genipin, geniposide had no effect upon combination with oxaliplatin (Supplementary Fig S1B and S1C). These results suggest that genipin enhances oxaliplatin sensitivity in colorectal cancer cells.

Table 1. Antibodies used for immunohistochemical staining

Antibody	Source	Catalog number	Dilution
BIM	Cell Signaling Technology	2933	1:100
SOD3	Santa Cruz Biotechnology	SC-58427	1:100

Abbreviation: SOD, superoxide dismutase.

Table 2. IHC scoring

Percentage score (PS)	Observation	Intensity score (IS)	Observation
1	0%–5%	0	None
2	6%–25%	1	White brown
3	26%–50%	2	Brown
4	51%–75%	3	Dark brown
5	76%–100%		

Genipin increased oxaliplatin-induced apoptosis in colorectal cancer cells

First, the combined effect of oxaliplatin and genipin on HCT116 cell morphology was examined under a light microscope. The morphology of cells treated with the combination was altered, compared with that of control cells or of cells treated with only genipin or oxaliplatin (Fig. 2A). We also confirmed the effect of oxaliplatin and genipin by *in vitro* bioluminescence imaging of HCT116-Luc cells. The combination of oxaliplatin and genipin inhibited cell viability to a greater extent than the control or either treatments alone (Fig. 2B). In addition, a colony formation assay was performed to detect the long-term effect of oxaliplatin and genipin combination on proliferation. The combination inhibited the colony-forming ability of cells better than the control or either treatments alone (Fig. 2C). To further investigate the mechanism of oxaliplatin–genipin synergism, we performed FACS analysis after annexin V/PI staining. The combination of oxaliplatin and genipin significantly enhanced apoptosis (Fig. 2D). Next, we calculated the combination index (CI) whether combination of oxaliplatin–genipin have synergistic effect by using CompuSyn software. As shown in Supplementary Fig. S1D, the combination of oxaliplatin and genipin had strong synergistic effect. We also measured the levels of cleaved PARP, caspase-9, and caspase-3, and the combination increased the levels of these proteins (Fig. 2E). To confirm these results, we pretreated cells with 25 μmol/L z-VAD-fmk for 30 minutes, a pan-caspase inhibitor, to determine whether the decrease in cell viability was due to caspase-dependent apoptosis. Activities of PARP and caspase-3, 9 induced by the combination of oxaliplatin and genipin were decreased by z-VAD-fmk (Fig. 2F). These results were also confirmed in DLD-1 cells (Supplementary Fig. S2). Our results indicate that the combination of oxaliplatin and genipin induces caspase-dependent apoptosis.

Genipin enhanced oxaliplatin-induced apoptosis by increasing BIM levels

To further investigate the mechanisms underlying genipin-mediated increase in oxaliplatin sensitivity, we quantified the expression of pro-apoptotic and anti-apoptotic proteins. We found that the expression of pro-apoptotic proteins, BIM and Bak, were significantly increased by genipin (Fig. 3A). However, the expression of anti-apoptotic Bcl-xL, XIAP, survivin, and Mcl-1 did not change. This genipin-induced change was also confirmed in DLD-1, SNU283, HT29, and SW48 cells (Fig. 3B). As shown

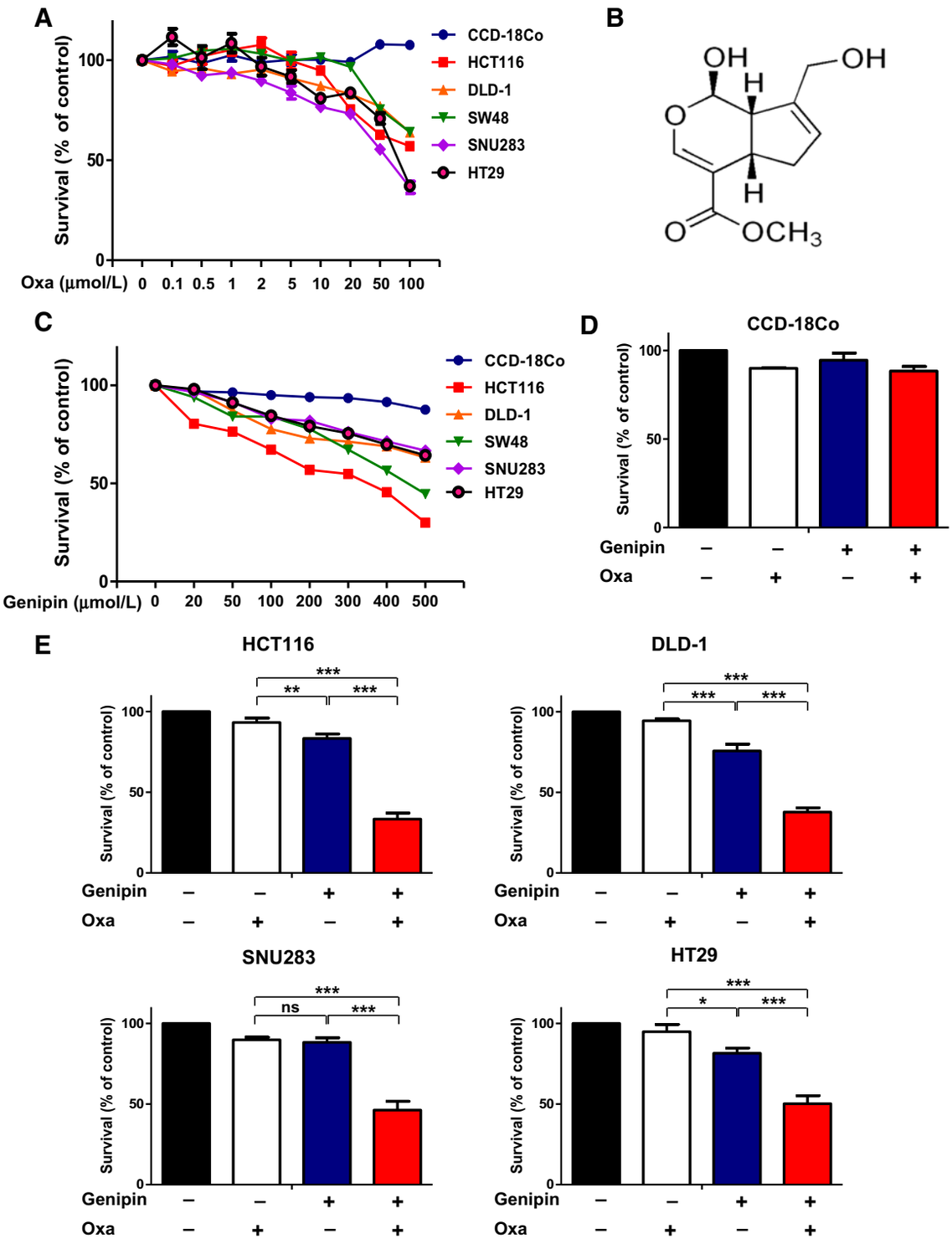

Figure 1.

Genipin enhanced oxaliplatin sensitivity in colorectal cancer (CRC) cells but not in normal primary colon cells. **A,** Treatment with 0–100 μmol/L oxaliplatin for 24 hours. **B,** Molecular structure of genipin. **C,** Cell viabilities of colorectal cancer and normal colon (CCD-18Co) cell lines were measured by using the MTT assay after treatment with 0–500 μmol/L genipin. **D** and **E,** Cell viabilities of colorectal cancer and CCD-18Co cell lines were measured by trypan blue dye staining after treatment with genipin, oxaliplatin, or their combination. Cells were incubated in the presence or absence of 10 μmol/L oxaliplatin and/or 100 μmol/L genipin for 24 hours. The data are expressed as the mean of three independent experiments. *, $P < 0.05$; **, $P < 0.01$; ***, $P < 0.001$. Oxa: oxaliplatin.

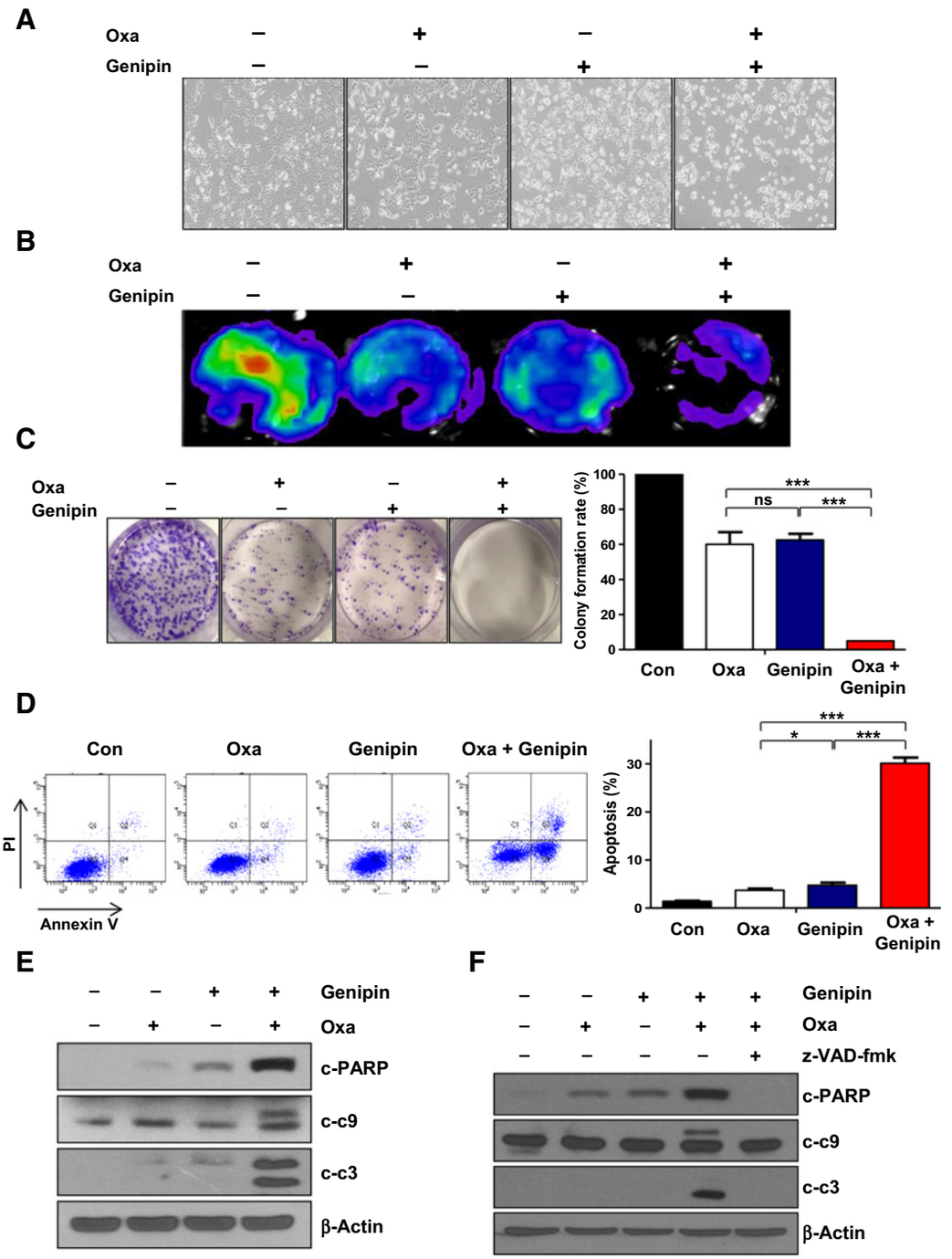

Figure 2.

Genipin increased oxaliplatin-induced apoptosis in colorectal cancer cells. **A,** HCT116 cells were treated with 10 μmol/L oxaliplatin, 100 μmol/L genipin, or their combination for 24 hours, and cell morphology was examined by light microscopy; scale bar, 100 μm. **B,** HCT116-Luc cells were treated with 10 μmol/L oxaliplatin, 100 μmol/L genipin, or their combination. After treatment with D-luciferin, cells were photographed using NightOWL LB983 *in vivo* bioluminescence imaging (BLI) system. **C,** HCT116 cells were treated with 10 μmol/L oxaliplatin, 100 μmol/L genipin, or their combination. After 14 days, the cells were stained with crystal violet dye, and photographs of the colonies were obtained using a digital camera (left). The graph shows the percentage of stained colonies (right). **D,** HCT116 cells were treated with 10 μmol/L oxaliplatin, 100 μmol/L genipin, or their combination, stained with annexin V and propidium iodide, and then analyzed with flow cytometry. *, $P < 0.05$; ***, $P < 0.001$. **E,** Levels of cleaved PARP, cleaved caspase-9, and cleaved caspase-3 were detected by western blotting. Equal loading was verified using β-actin. **F,** HCT116 cells were pretreated with 25 μmol/L z-VAD-fmk for 30 minutes, and then treated with 10 μmol/L oxaliplatin + 100 μmol/L genipin for 24 hours. Levels of cleaved PARP, cleaved caspase-9, and cleaved caspase-3 were detected by western blotting. Equal loading was verified using β-actin. The data are expressed as the mean of three independent experiments. Oxa: oxaliplatin, Con: control.

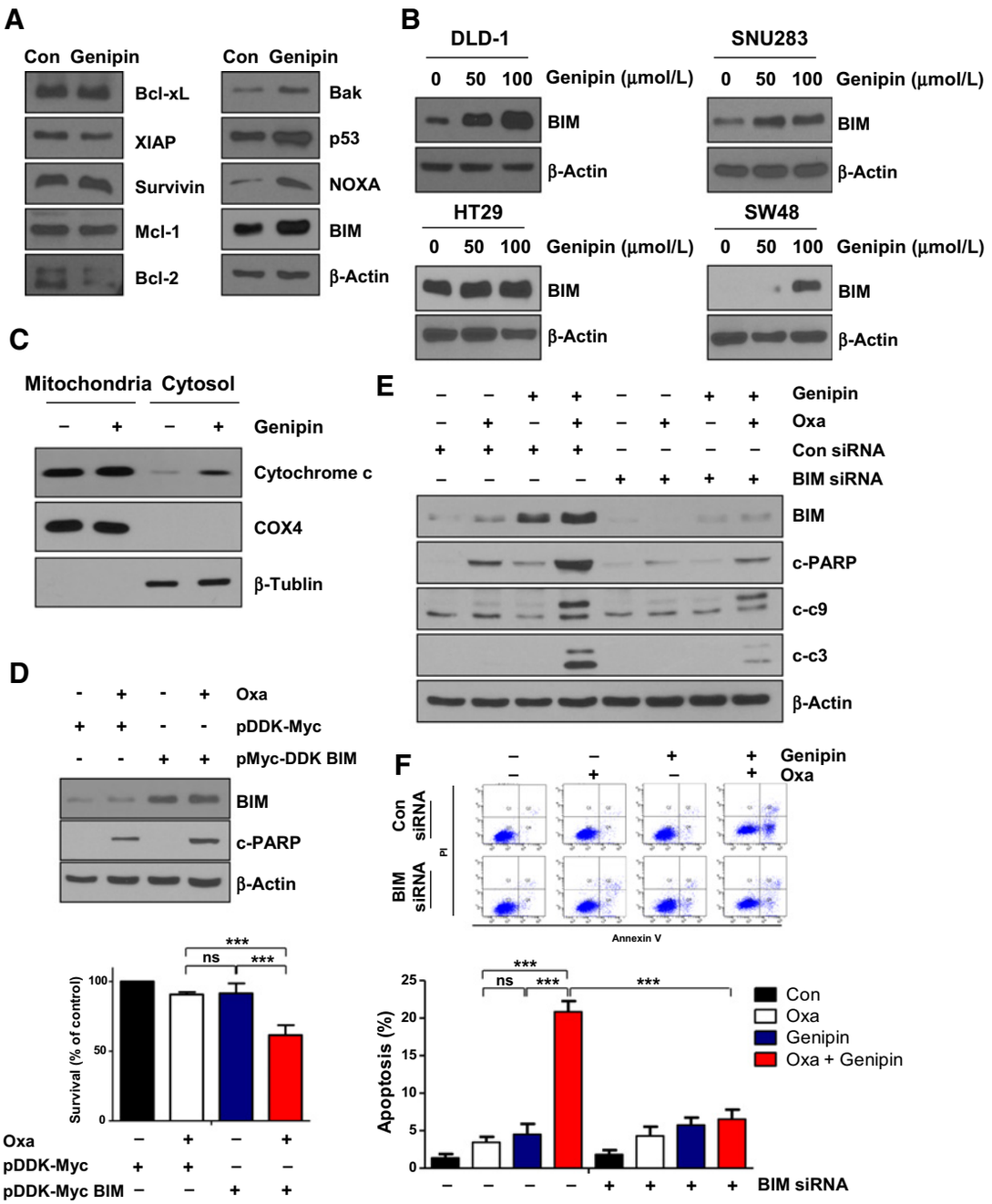

Figure 3.

Genipin enhanced oxaliplatin-induced apoptosis by increasing BIM levels. **A,** HCT116 cells were treated with 100 μmol/L genipin for 24 hours. The expression levels of pro-apoptotic proteins, such as Bak, p53, NOXA, and BIM, and anti-apoptotic proteins, such as Bcl-xL, XIAP, survivin, Mcl-1, and BCL-2, were measured by western blotting. Equal loading was verified using β-actin. **B,** DLD-1, SNU283, HT29, and SW48 cells were treated with genipin (0, 50, or 100 μmol/L) for 24 hours. The expression levels of BIM were measured by western blotting. Equal loading was verified using β-actin. **C,** HCT116 cells were treated with 100 μmol/L genipin for 24 hours. The expression level of Cytochrome c was detected by using western blotting. Proteins were normalized using β-tublin as a cytosolic fraction marker and COX4 as a mitochondrial fraction marker. **D,** HCT116 cells were transfected with the pCMV6-Myc-DDK BIM vector and then treated with 10 μmol/L oxaliplatin for 24 hours. The expression levels of BIM and cleaved PARP were detected by western blotting (top). Cell viabilities were evaluated by staining with trypan blue dye (bottom). **E,** HCT116 cells were transfected with control siRNA or BIM siRNA. The cells were then treated with 10 μmol/L oxaliplatin + 100 μmol/L genipin for 24 hours. The expression levels of BIM, cleaved PARP, cleaved caspase-9, and cleaved caspase-3 were detected by western blotting. Equal loading was verified using β-actin. **F,** HCT116 cells were transfected with control siRNA or BIM siRNA. The cells were then treated with 10 μmol/L oxaliplatin + 100 μmol/L genipin, stained with annexin V and propidium iodide, and then analyzed by flow cytometry. The data are expressed as the mean of three independent experiments. ***, $P < 0.001$. Oxa: oxaliplatin, Con: control.

in Fig. 3C, we also confirmed that genipin caused a release of cytochrome c from the mitochondria to the cytoplasm (Fig. 3C). We then transfected cells with pCMV6-Myc-DDK BIM to confirm the importance of BIM expression, which was found to be enhanced after exposure to oxaliplatin, thereby resulting in increased apoptosis (Fig. 3D). To further confirm whether oxaliplatin/genipin-induced apoptosis is BIM-dependent, we silenced BIM using BIM-specific siRNA. BIM knockdown decreased the apoptosis-inducing effect of oxaliplatin and genipin combination. Caspase-3, 9 activation and PARP cleavage was decreased by BIM siRNA (Fig. 3E). In addition, BIM knockdown significantly reduced apoptosis as measured by FACS analysis (Fig. 3F). These data indicate that genipin increases oxaliplatin sensitivity by upregulating BIM.

Genipin induced the activation of the ROS-endoplasmic reticulum stress-BIM pathway

Because endoplasmic reticulum (ER) stress is known to induce the expression of BIM, we tested whether genipin regulates ER stress proteins (18–20). Genipin increased p-IRE1α and p-JNK. However, other factors were not affected (Fig. 4A). To confirm whether BIM was increased by IRE1α-JNK, we pretreated cells with a JNK inhibitor (20 μmol/L). Apoptosis induced by oxaliplatin and genipin combination markedly decreased by JNK inhibition (Supplementary Fig. S3A). Because ROS is known to induce ER stress, we hypothesized that genipin-induced ROS causes ER stress. We measured the generation of ROS by DHE. Treatment with genipin significantly increased ROS (Fig. 4B). We also performed immunofluorescence analysis to measure the expression of DHE (Supplementary Fig. S3C). Genipin increased oxidative stress markers 3NT and 4HNE (Fig. 4C). To further examine whether ROS induced by genipin contributes to the synergistic effects of oxaliplatin and genipin combination, we pretreated cells with 5 mmol/L N-acetyl-L-cysteine (NAC; an antioxidant). The levels of apoptotic proteins increased by the combination were decreased by treatment with NAC (Fig. 4D). In addition, these results were confirmed by FACS analysis (Fig. 4E; Supplementary Fig. S3B). Finally, to investigate how genipin regulates ROS generation, we confirmed the expression of ROS-related factors, such as superoxide radical generating enzymes (NOX2 and NOX4) and anti-oxidative proteins (SOD1, 2, 3, and catalase). As shown in Fig. 4F and G; Supplementary Fig. S3D, genipin decreased the protein and mRNA levels of SOD3 via regulation of SOD3 transcription. SOD3 is mainly located on the plasma membrane and often secreted outside the cells. To examine whether HCT116 cells produce soluble forms of SOD3, cell-conditioned media and whole-cell lysates from HCT116 cells cultured in the presence or absence of genipin were subjected to western blotting with anti-SOD3. SOD3 was not secreted from the plasma membrane by genipin in colorectal cancer cells (Supplementary Fig. S3E). These results indicate that genipin inhibited SOD3 when it is already taken up by the cells. We also showed the overexpression of SOD3 in cells transfected with the pCMV6-Myc-DDK SOD3 vector to confirm the importance of SOD3 and its apoptotic effects. We found that the apoptotic proteins increased by the combination treatment were decreased by overexpression of SOD3 (Fig. 4H). These results suggest that genipin enhances oxaliplatin sensitivity by activating ROS-ER stress through inhibition of SOD3 mRNA expression.

Combination of oxaliplatin and genipin induced apoptosis *in vivo*

HCT116-Luc cells (3×10^6) were subcutaneously injected into BALB/c nude mice. When the size of the tumors was 100 mm^3, nude mice were randomized into four groups and treated with oxaliplatin and genipin at doses of 5 or 10 mg/kg every three days by intraperitoneal injection. The combination of oxaliplatin and genipin significantly decreased tumor growth and size compared with control or single treatments (Fig. 5A and B; Supplementary Fig. S4). In addition, tumor weight markedly decreased in the combination group compared with those in the other groups (Fig. 5C). Our results indicate that the combination of oxaliplatin and genipin synergistically reduces tumor size and weight. Next, we performed IHC to confirm the expression of SOD3 and BIM. Consistent with *in vitro* results, the expression of BIM was increased by genipin alone or in combination with oxaliplatin. Whereas, the expression of SOD3 was decreased by genipin or the combination (Fig. 5D). Finally, we carried out a TUNEL assay for detecting cell apoptosis. The combination of oxaliplatin and genipin increased TUNEL-positive cells compared with other treatments (Fig. 5E). Taken together, the combination of oxaliplatin and genipin enhanced apoptosis, and genipin may act as an oxaliplatin sensitizer.

Discussion

Recently, various studies focusing on increasing drug sensitivity of conventional chemotherapy by combining other agents, such as natural products, have been carried out. Because natural products from plants are safe and have low toxicity, they are ideal chemotherapy sensitizers for colorectal cancer therapy (21, 22).

In this study, we investigated whether genipin could act with oxaliplatin in a synergistic manner for treating colorectal cancer. Our results showed that the combination of oxaliplatin and genipin dramatically suppressed cell viability and induced caspase-dependent apoptosis in colorectal cancer cells; however, normal colon cells were less sensitive to this treatment (Fig. 1). In addition, the combination of oxaliplatin and genipin decreased tumor volume and enhanced apoptosis in a xenograft model (Fig. 5). Moreover, the dose of 5 mg/kg oxaliplatin is much lower than that administered to patients with colorectal cancer (24–26 mg, 85 mg/m^2; refs. 23–25). Combinations of compounds derived from other natural products and synthetic chemotherapeutic agents exhibit reduced toxicity (26, 27). Therefore, the combination of oxaliplatin and genipin may reduce the adverse effects of oxaliplatin and increase its cytotoxicity. The synergistic effect of this combination effect may be due to the upregulation of the pro-apoptotic protein BIM in colorectal cancer cell lines (DLD-1, SNU283, HT29, and SW48), as shown in Fig. 3.

Apoptosis has been reported to occur primarily through intrinsic and extrinsic pathways. Among them, the intrinsic pathway is regulated by the balance between pro-apoptotic proteins (Bax, Bak, and BIM) and anti-apoptotic proteins (Bcl-xL and Bcl-2) of the Bcl-2 family (28, 29). The upregulation of BIM triggers cytochrome c release from the mitochondria, induces the formation of apoptosomes, and the activation of caspase-3 (30). Thus, the upregulation of BIM induces apoptosis.

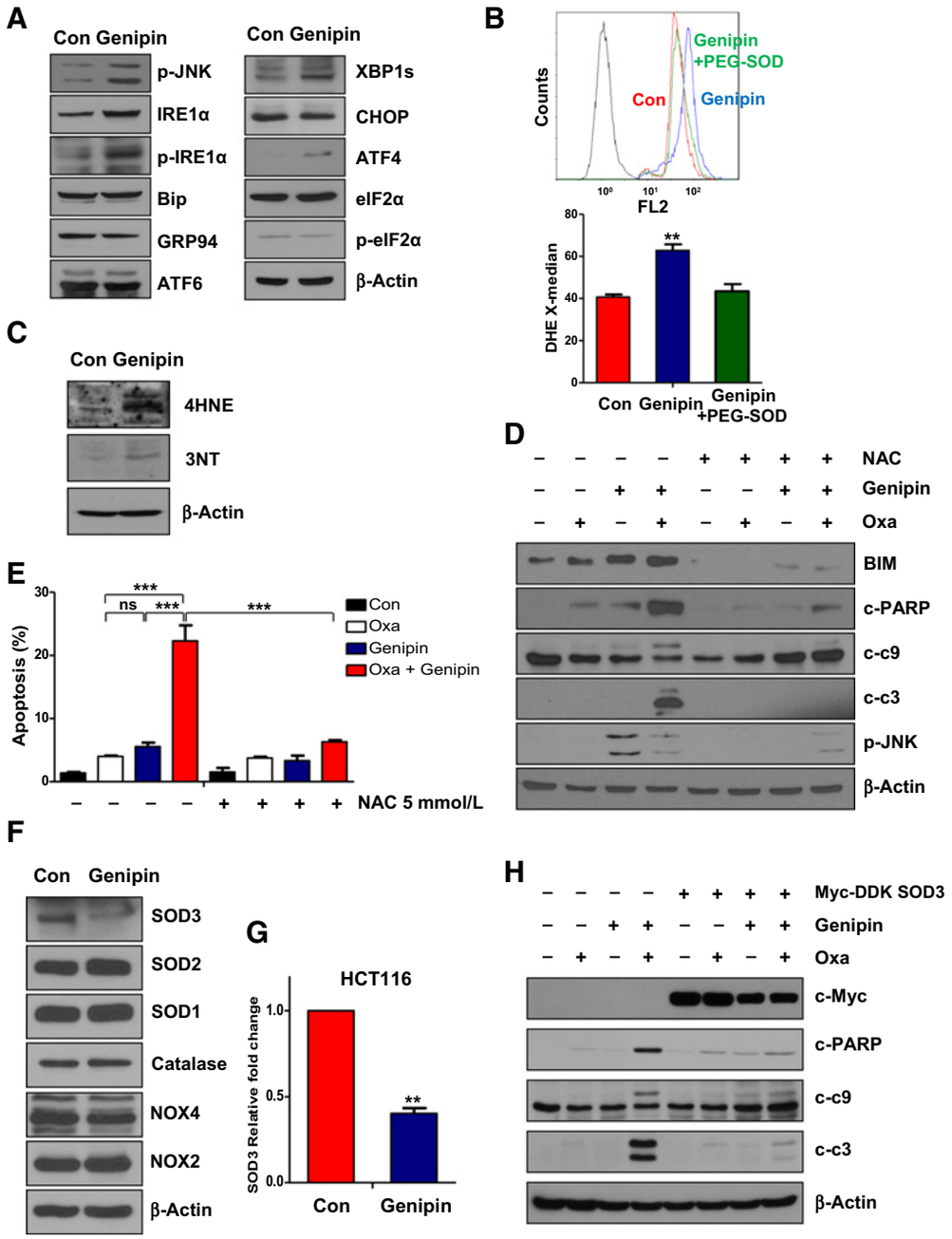

Figure 4.

Genipin induced the activation of the ROS-endoplasmic reticulum (ER) stress-BIM pathway. **A,** HCT116 cells were treated with 100 μmol/L genipin for 24 hours. The expression levels of p-JNK, IRE1α, p-IRE1α, Bip, GRP94, ATF6, XBP1s, CHOP, ATF4, eIF2α, and p-eIF2α (ER stress) were detected by western blotting. Equal loading was verified using β-actin. **B,** HCT116 cells were treated with genipin or PEG-SOD (100 U/mL). The expression levels of ROS were measured by DHE staining and analyzed by flow cytometry. **C,** HCT116 cells were treated with 100 μmol/L genipin for 24 hours. The expression levels of oxidative damage products 4HNE, 3NT were measured by western blotting. Equal loading was verified using β-actin. **D,** HCT116 cells were pretreated with 5 mmol/L NAC for 1 hours, and then treated with 10 μmol/L oxaliplatin + 100 μmol/L genipin for 24 hours. The expression levels of BIM, cleaved PARP, cleaved caspase-9, cleaved caspase-3, and p-JNK were detected by western blotting. Equal loading was verified using β-actin. **E,** HCT116 cells were pretreated with 5 mmol/L NAC for 1 hour, and then treated with 10 μmol/L oxaliplatin + 100 μmol/L genipin for 24 hours. The cells were stained with annexin V and propidium iodide, and then analyzed by flow cytometry. ***, $P < 0.001$. **F,** HCT116 cells were treated with 100 μmol/L genipin for 24 hours. The expression levels of SOD1, SOD2, SOD3, catalase, NOX2, and NOX4 were measured by western blotting. Equal loading was verified using β-actin. **G,** The mRNA level of *SOD3* was measured by using real time PCR. The expression was normalized to that of GAPDH. **H,** HCT116 cells were transfected with Myc-DDK SOD3. The expression levels of c-Myc, cleaved PARP, cleaved caspase-9, and cleaved caspase-3 were measured by using western blotting. The data are expressed as the mean of three independent experiments. ***, $P < 0.001$. Oxa: oxaliplatin, Con: control, NAC: N-acetyl-L-cysteine, SOD: superoxide dismutase.

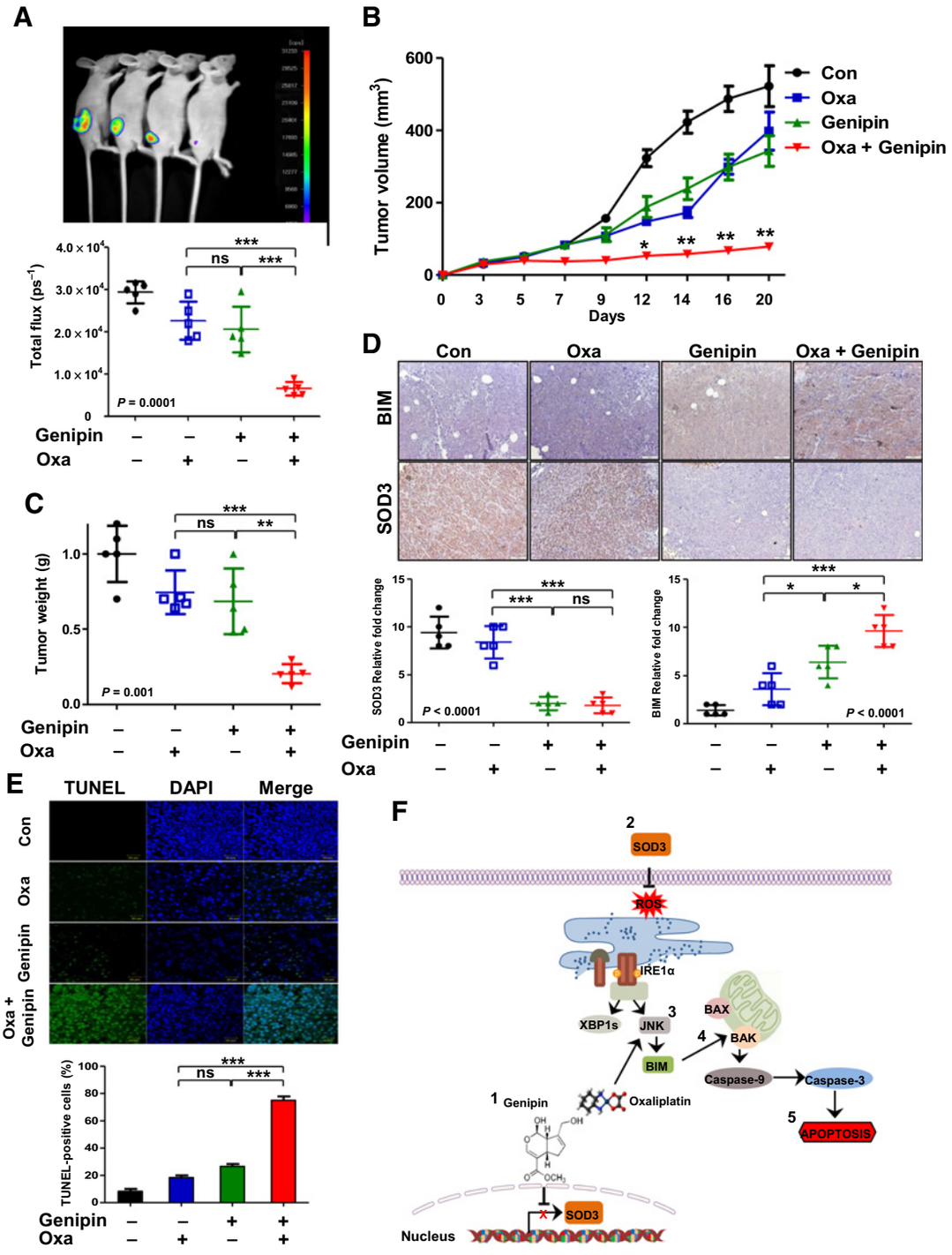

Figure 5.

Combination of oxaliplatin and genipin induced apoptosis *in vivo*. **A,** HCT116-luc cells were implanted subcutaneously in nude mice, and tumor growth was measured every 2 days based on fluorescence intensity after 3 weeks of treatment with 10 mg/kg genipin, 5 mg/kg oxaliplatin, or their combination ($n = 5$). **B,** The graph shows tumor volume in xenograft nude mice. Tumor volumes were determined by caliper measurements every 2 days. **C,** After concluding the experiment, the tumor weight of each mouse was measured. **D,** Immunohistochemistry (IHC) staining results of BIM and SOD3 on tumor sections from xenograft mice of the four groups at a magnification of ×20; scale bar, 50 μm. The graph shows the expression of BIM and SOD3 by IHC staining. **E,** The detection of apoptosis in xenograft mice tumors by TUNEL assay, and the nucleus was stained with DAPI (top). The percentage of TUNEL-positive cells was counted and plotted as a histogram (bottom). **F,** Schematic representation of genipin-mediated enhancement in oxaliplatin-induced apoptosis. The data are expressed as the mean of three independent experiments. *, $P < 0.05$; **, $P < 0.01$; ***, $P < 0.001$. Oxa: oxaliplatin, Con: control, SOD: superoxide dismutase.

Our results also showed that BIM is important for increasing oxaliplatin sensitivity. BIM knockdown decreased genipin-induced increase in oxaliplatin sensitivity (Fig. 3E and F).

The ER plays a key role in the regulation of protein synthesis, folding, and trafficking (31, 32). ER stress occurs when a number of unfolded proteins are produced in the ER lumen (33, 34). Stressful environmental conditions can trigger the activation of unfolded proteins in cells and the expression of ER stress-related genes (Fig. 4A). ER stress is reported to induce the activation of BIM via IRE1α/JNK, IRE1α/CHOP, or PERK/ATF4/CHOP pathways (18, 35). Usually, ER stress is induced by oxidative agents that modulate cancer cell survival (36). Consistent with these reports, we found that ER stress induced by genipin markedly upregulates BIM by inducing the IRE1α/JNK/BIM pathway in colorectal cancer cell lines. In addition, we found that an increase in BIM by ER stress is associated with an increased generation of ROS. ROS plays an important role in the initiation and progression of cancer. Because cancer cells have a higher ROS level than normal cells, they are vulnerable to the acute induction of oxidative stress (37). Excessive ROS can be toxic to cancer cells, which can ultimately lead to their necrosis or apoptosis (38). In addition, ROS is known to induce ER stress (39). Our results show that genipin induces ROS generation, and the quenching of ROS by NAC attenuates genipin-mediated increase in BIM and JNK. NAC has protective effects on carcinogenesis and DNA damage, which are involved in antioxidant activity. This link correlates with the amount of ROS and DNA damage produced by the platinum agents (cisplatin and oxaliplatin) that are being used in anticancer drugs (40, 41). In other words, antioxidants (NAC, thiosulfate, and glutathione) can be act as reducing agents that covalent bond to electrophilic compounds (platinum-based) such as oxaliplatin, cisplatin, and mixing oxaliplatin or cisplatin with thiosulfate prior to treatment inhibits the anticancer agent's (42). Furthermore, once in the cell, platinum-based compounds such as oxaliplatin and cisplatin are rapidly bound to cytoplasmatic proteins, among which antioxidant proteins like reduced glutathione (43) and inducing mitochondrial dysfunction (44). The quenching of ROS decreased cell death induced by oxaliplatin and genipin combination. Thus, these results indicate that genipin-induced ROS, plays a role in oxaliplatin sensitivity. ROS is produced by mitochondria and NADPH oxidase (45). ROS is regulated by SOD that catalyzes the dismutation of the superoxide (O_2^-) radical into oxygen and H_2O_2. Cytoplasmic Cu/ZnSOD (SOD1), mitochondrial MnSOD (SOD2), and extracellular Cu/ZnSOD (SOD3) are all cellular antioxidants (45, 46). We measured the expression of NOXs and SODs to investigate how genipin regulates ROS. Treatment with genipin decreased the protein and mRNA expression of SOD3. However, the expression of SOD1, SOD2, catalase, NOX2, and NOX4 did not change (Fig. 4F and G).

In the previous study, we found that genipin induced apoptosis by inhibiting the sonic hedgehog pathway (15). We tested whether decrease of SOD3 mRNA induced by genipin depends on hedgehog pathway. The mRNA of SOD3 was decreased by genipin in both cell lines, expressing (HCT116) or not expressing (DLD-1) the hedgehog transcription factor Gli-1 (Fig 4G; Supplementary Fig. S3D). The downregulation of SOD3 induces apoptosis through ROS generation (38, 47). Accordingly, reduction in SOD3 level led to ROS-mediated apoptosis. In conclusion, our results demonstrate that the combination of oxaliplatin and genipin induces significant synergistic effects *in vitro* and *in vivo* compared with individual treatments in colorectal cancer cell lines. This synergism was based on an increased apoptotic potential owing to the activation of the ROS/ER stress/BIM signaling pathway (Fig. 5F). Currently, combination therapies including more than 30 natural compounds are undergoing clinical trials for cancer treatment. Thus, the findings of our study may be investigated further through preclinical trials. Taken together, our study supports the preclinical evidence that the combination of oxaliplatin and genipin could be a novel therapeutic strategy for the treatment of colorectal cancer.

Disclosure of Potential Conflicts of Interest

No potential conflicts of interest were disclosed.

Authors' Contributions

Conception and design: B.R. Kim, Y.A. Jeong, D.-H. Lee, S.C. Oh
Development of methodology: B.R. Kim, Y.A. Jeong, S.H. Park, S.C. Oh
Acquisition of data (provided animals, acquired and managed patients, provided facilities, etc.): B.R. Kim, Y.A. Jeong
Analysis and interpretation of data (e.g., statistical analysis, biostatistics, computational analysis): B.R. Kim, Y.A. Jeong, M.J. Jo, S. Jeong, H.K. Yun, S. Kang, D.-H. Lee, S.C. Oh
Writing, review, and/or revision of the manuscript: B.R. Kim, Y.A. Jeong, Y.J. Na, S.C. Oh
Administrative, technical, or material support (i.e., reporting or organizing data, constructing databases): B.R. Kim, Y.A. Jeong, J.L. Kim, S.C. Oh
Study supervision: D.-H. Lee, S.C. Oh

Acknowledgments

This work was supported by the National Research Foundation (NRF) of Korea grant funded by the Korean government (MSIP; NRF-2017R1A6A3A11030765) and [NRF-2017R1A2B2011684] and supported by a Korea University Grant.

The costs of publication of this article were defrayed in part by the payment of page charges. This article must therefore be hereby marked *advertisement* in accordance with 18 U.S.C. Section 1734 solely to indicate this fact.

Received February 21, 2018; revised July 12, 2018; accepted February 4, 2019; published first February 20, 2019.

References

1. Ferlay J, Soerjomataram I, Dikshit R, Eser S, Mathers C, Rebelo M, et al. Cancer incidence and mortality worldwide: sources, methods and major patterns in GLOBOCAN 2012. Int J Cancer 2015;136:E359–86.
2. Edwards BK, Noone AM, Mariotto AB, Simard EP, Boscoe FP, Henley SJ, et al. Annual Report to the Nation on the status of cancer, 1975–2010, featuring prevalence of comorbidity and impact on survival among persons with lung, colorectal, breast, or prostate cancer. Cancer 2014; 120:1290–314.
3. Figueredo A, Charette ML, Maroun J, Brouwers MC, Zuraw L. Adjuvant therapy for stage II colon cancer: a systematic review from the Cancer Care Ontario Program in evidence-based care's gastrointestinal cancer disease site group. J Clin Oncol 2004;22:3395–407.
4. Gill S, Loprinzi CL, Sargent DJ, Thome SD, Alberts SR, Haller DG, et al. Pooled analysis of fluorouracil-based adjuvant therapy for stage II and III colon cancer: who benefits and by how much? J Clin Oncol 2004;22: 1797–806.
5. Lee KH, Kim MK, Kim YH, Ryoo BY, Lim HY, Song HS, et al. Gemcitabine and oxaliplatin combination as first-line treatment for advanced pancreatic cancer: a multicenter phase II study. Cancer Chemother Pharmacol 2009; 64:317–25.

6. Kelland L. The resurgence of platinum-based cancer chemotherapy. Nat Rev Cancer 2007;7:573–84.
7. Faivre S, Chan D, Salinas R, Woynarowska B, Woynarowski JM. DNA strand breaks and apoptosis induced by oxaliplatin in cancer cells. Biochem Pharmacol 2003;66:225–37.
8. Andre T, Boni C, Navarro M, Tabernero J, Hickish T, Topham C, et al. Improved overall survival with oxaliplatin, fluorouracil, and leucovorin as adjuvant treatment in stage II or III colon cancer in the MOSAIC trial. J Clin Oncol 2009;27:3109–16.
9. Pelzer U, Schwaner I, Stieler J, Adler M, Seraphin J, Dorken B, et al. Best supportive care (BSC) versus oxaliplatin, folinic acid and 5-fluorouracil (OFF) plus BSC in patients for second-line advanced pancreatic cancer: a phase III-study from the German CONKO-study group. Eur J Cancer 2011; 47:1676–81.
10. Muzzarelli RA, El Mehtedi M, Bottegoni C, Gigante A. Physical properties imparted by genipin to chitosan for tissue regeneration with human stem cells: a review. Int J Biol Macromol 2016;93:1366–81.
11. Austero MS, Donius AE, Wegst UG, Schauer CL. New crosslinkers for electrospun chitosan fibre mats. I. Chemical analysis. J R Soc Interface 2012;9:2551–62.
12. Nam KN, Choi YS, Jung HJ, Park GH, Park JM, Moon SK, et al. Genipin inhibits the inflammatory response of rat brain microglial cells. Int Immunopharmacol 2010;10:493–9.
13. Tanaka M, Yamazaki M, Chiba K. Neuroprotective action of genipin on tunicamycin-induced cytotoxicity in neuro2a cells. Biol Pharm Bull 2009; 32:1220–3.
14. Feng Q, Cao HL, Xu W, Li XR, Ren YQ, Du LF. Apoptosis induced by genipin in human leukemia K562 cells: involvement of c-Jun N-terminal kinase in G(2)/M arrest. Acta Pharmacol Sin 2011;32:519–27.
15. Kim BR, Jeong YA, Na YJ, Park SH, Jo MJ, Kim JL, et al. Genipin suppresses colorectal cancer cells by inhibiting the Sonic Hedgehog pathway. Oncotarget 2017;8:101952–64.
16. Han Z, Boyle DL, Chang L, Bennett B, Karin M, Yang L, et al. c-Jun N-terminal kinase is required for metalloproteinase expression and joint destruction in inflammatory arthritis. J Clin Invest 2001;108: 73–81.
17. Bennett BL, Sasaki DT, Murray BW, O'Leary EC, Sakata ST, Xu W, et al. SP600125, an anthrapyrazolone inhibitor of Jun N-terminal kinase. Proc Natl Acad Sci U S A 2001;98:13681–6.
18. Deldicque L. Endoplasmic reticulum stress in human skeletal muscle: any contribution to sarcopenia? Front Physiol 2013;4:236.
19. Cheng H, Force T. Molecular mechanisms of cardiovascular toxicity of targeted cancer therapeutics. Circ Res 2010;106:21–34.
20. Doyle KM, Kennedy D, Gorman AM, Gupta S, Healy SJ, Samali A. Unfolded proteins and endoplasmic reticulum stress in neurodegenerative disorders. J Cell Mol Med 2011;15:2025–39.
21. Fulda S, Debatin KM. Sensitization for tumor necrosis factor-related apoptosis-inducing ligand-induced apoptosis by the chemopreventive agent resveratrol. Cancer Res 2004;64:337–46.
22. Zhang Y, Li Q, Wang J, Cheng F, Huang X, Cheng Y, et al. Polysaccharide from Lentinus edodes combined with oxaliplatin possesses the synergy and attenuation effect in hepatocellular carcinoma. Cancer Lett 2016;377: 117–25.
23. Di Bartolomeo M, Ciarlo A, Bertolini A, Barni S, Verusio C, Aitini E, et al. Capecitabine, oxaliplatin and irinotecan in combination, with bevacizumab (COI-B regimen) as first-line treatment of patients with advanced colorectal cancer. An Italian Trials of Medical Oncology phase II study. Eur J Cancer 2015;51:473–81.
24. Kho Y, Jansman FG, Prins NH, Neef C, Brouwers JR. Population pharmacokinetics of oxaliplatin (85 mg/m2) in combination with 5-fluorouracil in patients with advanced colorectal cancer. Ther Drug Monit 2006;28: 206–11.
25. Moreno-Solorzano I, Ibeas-Rollan R, Monzo-Planella M, Moreno-Solorzano J, Martinez-Rodenas F, Pou-Sanchis E, et al. Two Doses of oxaliplatin with capecitabine (XELOX) in metastatic colorectal cancer. Clin Colorectal Cancer 2007;6:634–40.
26. Das R, Bhattacharya K, Sarkar S, Samanta SK, Pal BC, Mandal C. Mahanine synergistically enhances cytotoxicity of 5-fluorouracil through ROS-mediated activation of PTEN and p53/p73 in colon carcinoma. Apoptosis 2014;19:149–64.
27. Demain AL, Vaishnav P. Natural products for cancer chemotherapy. Microb Biotechnol 2011;4:687–99.
28. Taylor RC, Cullen SP, Martin SJ. Apoptosis: controlled demolition at the cellular level. Nat Rev Mol Cell Biol 2008;9:231–41.
29. Ichim G, Tait SW. A fate worse than death: apoptosis as an oncogenic process. Nat Rev Cancer 2016;16:539–48.
30. O'Connor L, Strasser A, O'Reilly LA, Hausmann G, Adams JM, Cory S, et al. Bim: a novel member of the Bcl-2 family that promotes apoptosis. EMBO J 1998;17:384–95.
31. Stephens SB, Nicchitta CV. Divergent regulation of protein synthesis in the cytosol and endoplasmic reticulum compartments of mammalian cells. Mol Biol Cell 2008;19:623–32.
32. Araki K, Nagata K. Protein folding and quality control in the ER. Cold Spring Harb Perspect Biol 2011;3:a007526.
33. Xu C, Bailly-Maitre B, Reed JC. Endoplasmic reticulum stress: cell life and death decisions. J Clin Invest 2005;115:2656–64.
34. Sano R, Reed JC. ER stress-induced cell death mechanisms. Biochim Biophys Acta 2013;1833:3460–70.
35. Kim I, Xu W, Reed JC. Cell death and endoplasmic reticulum stress: disease relevance and therapeutic opportunities. Nat Rev Drug Discov 2008;7: 1013–30.
36. Kapur A, Felder M, Fass L, Kaur J, Czarnecki A, Rathi K, et al. Modulation of oxidative stress and subsequent induction of apoptosis and endoplasmic reticulum stress allows citral to decrease cancer cell proliferation. Sci Rep 2016;6:27530.
37. Trachootham D, Alexandre J, Huang P. Targeting cancer cells by ROS-mediated mechanisms: a radical therapeutic approach? Nat Rev Drug Discov 2009;8:579–91.
38. Circu ML, Aw TY. Reactive oxygen species, cellular redox systems, and apoptosis. Free Radic Biol Med 2010;48:749–62.
39. Zeeshan HM, Lee GH, Kim HR, Chae HJ. Endoplasmic reticulum stress and associated ROS. Int J Mol Sci 2016;17:327.
40. Kelley MR, Jiang Y, Guo C, Reed A, Meng H, Vasko MR. Role of the DNA base excision repair protein, APE1 in cisplatin, oxaliplatin, or carboplatin induced sensory neuropathy. PLoS One 2014;9: e106485.
41. De Flora S, Izzotti A, D'Agostini F, Balansky RM. Mechanisms of N-acetylcysteine in the prevention of DNA damage and cancer, with special reference to smoking-related end-points. Carcinogenesis 2001;22: 999–1013.
42. Conklin KA. Dietary antioxidants during cancer chemotherapy: impact on chemotherapeutic effectiveness and development of side effects. Nutr Cancer 2000;37:1–18.
43. Hagrman D, Goodisman J, Souid AK. Kinetic study on the reactions of platinum drugs with glutathione. J Pharmacol Exp Ther 2004;308: 658–66.
44. Garrido N, Perez-Martos A, Faro M, Lou-Bonafonte JM, Fernandez-Silva P, Lopez-Perez MJ, et al. Cisplatin-mediated impairment of mitochondrial DNA metabolism inversely correlates with glutathione levels. Biochem J 2008;414:93–102.
45. Lambeth JD. NOX enzymes and the biology of reactive oxygen. Nat Rev Immunol 2004;4:181–9.
46. Zelko IN, Mariani TJ, Folz RJ. Superoxide dismutase multigene family: a comparison of the CuZn-SOD (SOD1), Mn-SOD (SOD2), and EC-SOD (SOD3) gene structures, evolution, and expression. Free Radic Biol Med 2002;33:337–49.
47. Laukkanen MO. Extracellular superoxide dismutase: growth promoter or tumor suppressor? Oxid Med Cell Longev 2016;2016:3612589.